Finger-Knuckle-Print Recognition Using BLPOC-Based Local Block Matching

Shoichiro Aoyama, Koichi Ito and Takafumi Aoki
Graduate School of Information Sciences, Tohoku University
6-6-05, Aramaki Aza Aoba, Sendai, 980–8579, Japan
Email: aoyama@aoki.ecei.tohoku.ac.jp

***Abstract*—This paper proposes a Finger-Knuckle-Print (FKP) recognition algorithm using Band-Limited Phase-Only Correlation (BLPOC)-based local block matching. The phase information obtained from 2D Discrete Fourier Transform (DFT) of images contains important information of image representation. The phase-based image matching, especially BLPOC-based image matching is successfully applied to image recognition tasks for biometric authentication applications. To calculate the matching score, the proposed algorithm corrects the global and local distortion between FKP images using the BLPOC-based local block matching. Experimental evaluation using the PolyU FKP database demonstrates efficient recognition performance of the proposed algorithm compared with the conventional algorithms.**

***Index Terms*—finger-knuckle-print, biometrics, phase-only correlation, local block matching**

I. Introduction

Biometric authentication has been receiving extensive attention with the need for robust human recognition techniques in various networked applications [1]. Biometric authentication (or simply biometrics) is to identify a person based on the physiological or behavioral characteristics such as fingerprint, face, iris, voice, signature, etc.

Among many biometric techniques, hand-based biometrics has been attracted lots of attention over past decade. Fingerprint [2], palmprint [3], [4], hand geometry [5], finger-knuckle-print [6], [7], [8], [9], [10], [11], and combinations of the above traits [12], [13], [14] have been used as biometric traits related to a hand. In this paper, we focus on recognizing a person using the Finger-Knuckle-Print (FKP) patterns.

So far, some works on FKP recognition has been reported. Woodard, et al. [6], it is the first attempt to use FKP for biometric authentication, have proposed a curvature-based recognition algorithm using 3D finger surface taken by a 3D sensor. The use of the 3D sensor is not acceptable for practical use due to its size, cost, weight, processing time, etc. On the other hand, the use of 2D FKP images makes it possible to realize compact and powerful biometric authentication systems. Kumar, et al. [9] have proposed a coding-based algorithm called KnuckleCode generated by using local Radon transform. Zhang, et al., have proposed some FKP recognition algorithms using the competitive code generated by using Gabor filter bank [7], BLPOC (Band-Limited Phase-Only Correlation) [8], combination of improved competitive code and magnitude code [10] and combination of competitive code and BLPOC [11]. The recognition performance of these algorithms is degraded for FKP images having nonlinear distortion due to movement of a finger, since these algorithms consider only rigid body transformation of FKP images.

In this paper, we propose a FKP recognition algorithm using BLPOC-based local block matching. In order to handle the nonlinear distortion of FKP images, the proposed algorithm corrects the global and local distortion of FKP images. The proposed algorithm corrects the affine transformation between FKP images estimated with the reliable correspondence obtained using the BLPOC-based local block matching, and then corrects translational displacement for each local image block pair using the BLPOC-based local block matching. Finally, we can calculate the reliable matching score for distortion-corrected local block images. Experimental evaluation using the PolyU FKP Database [15] demonstrates efficient recognition performance of the proposed algorithm compared with conventional algorithms.

II. Phase-Based Correspondence Matching

A. Phase-Only Correlation (POC)

We introduce the principle of a Phase-Only Correlation (POC) function (which is sometimes called the "phase-correlation function") [16], [17], [18].

Consider two $N_1 \times N_2$ images, $f(n_1, n_2)$ and $g(n_1, n_2)$, where we assume that the index ranges are $n_1 = -M_1, \cdots, M_1$ ($M_1 > 0$) and $n_2 = -M_2, \cdots, M_2$ ($M_2 > 0$) for mathematical simplicity, and hence $N_1 = 2M_1 + 1$ and $N_2 = 2M_2 + 1$. The discussion could be easily generalized to non-negative index ranges with power-of-two image size. Let $F(k_1, k_2)$ and $G(k_1, k_2)$ denote the 2D DFTs of the two images. $F(k_1, k_2)$ is given by

$$\begin{aligned} F(k_1, k_2) &= \sum_{n_1, n_2} f(n_1, n_2) W_{N_1}^{k_1 n_1} W_{N_2}^{k_2 n_2} \\ &= A_F(k_1, k_2) e^{j\theta_F(k_1, k_2)}, \end{aligned} \tag{1}$$

where $k_1 = -M_1, \cdots, M_1$, $k_2 = -M_2, \cdots, M_2$, $W_{N_1} = e^{-j\frac{2\pi}{N_1}}$, $W_{N_2} = e^{-j\frac{2\pi}{N_2}}$, and $\sum_{n_1, n_2}$ denotes $\sum_{n_1=-M_1}^{M_1} \sum_{n_2=-M_2}^{M_2}$. $A_F(k_1, k_2)$ is amplitude and $\theta_F(k_1, k_2)$ is phase. $G(k_1, k_2)$ is defined in the same way. The cross-phase spectrum $R_{FG}(k_1, k_2)$ is given by

$$R_{FG}(k_1, k_2) = \frac{F(k_1, k_2)\overline{G(k_1, k_2)}}{|F(k_1, k_2)\overline{G(k_1, k_2)}|} = e^{j\theta(k_1, k_2)}, \tag{2}$$

978-1-4577-0121-4/11/$26.00 ©2011 IEEE

where $\overline{G(k_1,k_2)}$ is the complex conjugate of $G(k_1,k_2)$ and $\theta(k_1,k_2)$ denotes the phase difference $\theta_F(k_1,k_2)-\theta_G(k_1,k_2)$. The POC function $r_{fg}(n_1,n_2)$ is the 2D Inverse DFT (2D IDFT) of $R_{FG}(k_1,k_2)$ and is given by

$$r_{fg}(n_1,n_2)=\frac{1}{N_1N_2}\sum_{k_1,k_2} R_{FG}(k_1,k_2)W_{N_1}^{-k_1n_1}W_{N_2}^{-k_2n_2}, \tag{3}$$

where $\sum_{k_1,k_2}$ denotes $\sum_{k_1=-M_1}^{M_1}\sum_{k_2=-M_2}^{M_2}$. When two images are similar, their POC function gives a distinct sharp peak. When two images are not similar, the peak drops significantly. The height of the peak gives a good similarity measure for image matching, and the location of the peak shows the translational displacement between the images.

B. Band-Limited POC (BLPOC)

We have proposed a BLPOC (Band-Limited Phase-Only Correlation) function [19] dedicated to biometric authentication tasks. The idea to improve the matching performance is to eliminate meaningless high frequency components in the calculation of cross-phase spectrum R_{FG} depending on the inherent frequency components of palmprint images. Assume that the ranges of the inherent frequency band are given by $k_1=-K_1,\cdots,K_1$ and $k_2=-K_2,\cdots,K_2$, where $0\leq K_1\leq M_1$ and $0\leq K_2\leq M_2$. Thus, the effective size of frequency spectrum is given by $L_1=2K_1+1$ and $L_2=2K_2+1$. The BLPOC function is given by

$$\begin{aligned} r_{fg}^{K_1K_2}(n_1,n_2) &= \frac{1}{L_1L_2}{\sum_{k_1,k_2}}' R_{FG}(k_1,k_2) \\ &\quad W_{L_1}^{-k_1n_1}W_{L_2}^{-k_2n_2}, \end{aligned} \tag{4}$$

where $n_1=-K_1,\cdots,K_1$, $n_2=-K_2,\cdots,K_2$, and $\sum'_{k_1,k_2}$ denotes $\sum_{k_1=-K_1}^{K_1}\sum_{k_2=-K_2}^{K_2}$. Note that the maximum value of the correlation peak of the BLPOC function is always normalized to 1 and does not depend on L_1 and L_2.

C. Phase-based correspondence matching

In order to handle the nonlinear distortion of FKP images, we employ the sub-pixel correspondence matching [18] using POC, which employs a coarse-to-fine strategy using image pyramids for robust correspondence search. Let $\boldsymbol{p}$ be a coordinate vector of a reference pixel in the reference image $I(n_1,n_2)$. The problem of sub-pixel correspondence search is to find a real-number coordinate vector $\boldsymbol{q}$ in the input image $J(n_1,n_2)$ that corresponds to the reference pixel $\boldsymbol{p}$ in $I(n_1,n_2)$. We briefly explain the procedure as follows.

Step 1: For $l=1,2,\cdots,l_{max}$, create the l-th layer images $I_l(n_1,n_2)$ and $J_l(n_1,n_2)$, i.e., coarser versions of $I_0(n_1,n_2)$ and $J_0(n_1,n_2)$, recursively as follows:

$$\begin{aligned} I_l(n_1,n_2) &= \frac{1}{4}\sum_{i_1=0}^{1}\sum_{i_2=0}^{1} I_{l-1}(2n_1+i_1,2n_2+i_2), \\ J_l(n_1,n_2) &= \frac{1}{4}\sum_{i_1=0}^{1}\sum_{i_2=0}^{1} J_{l-1}(2n_1+i_1,2n_2+i_2). \end{aligned}$$

Step 2: For every layer $l=1,2,\cdots,l_{max}$, calculate the coordinate $\boldsymbol{p}_l=(p_{l1},p_{l2})$ corresponding to the original reference point $\boldsymbol{p}_0$ recursively as follows:

$$\boldsymbol{p}_l = \lfloor \tfrac{1}{2}\boldsymbol{p}_{l-1}\rfloor = (\lfloor \tfrac{1}{2}p_{l-1\ 1}\rfloor, \lfloor \tfrac{1}{2}p_{l-1\ 2}\rfloor), \tag{5}$$

where $\lfloor z\rfloor$ denotes the operation to round the element of z to the nearest integer towards minus infinity.

Step 3: We assume that $\boldsymbol{q}_{l_{max}}=\boldsymbol{p}_{l_{max}}$ in the coarsest layer. Let $l=l_{max}-1$.

Step 4: From the l-th layer images $I_l(n_1,n_2)$ and $J_l(n_1,n_2)$, extract two sub-images (or image blocks) $f_l(n_1,n_2)$ and $g_l(n_1,n_2)$ with their centers on $\boldsymbol{p}_l$ and $2\boldsymbol{q}_{l+1}$, respectively. The size of image blocks is $W\times W$ pixels. In this paper, we employ $W=32$.

Step 5: Estimate the displacement between $f_l(n_1,n_2)$ and $g_l(n_1,n_2)$ with pixel accuracy using POC-based image matching. Let the estimated displacement vector be $\boldsymbol{\delta}_l$. The l-th layer correspondence $\boldsymbol{q}_l$ is determined as follows:

$$\boldsymbol{q}_l = 2\boldsymbol{q}_{l+1}+\boldsymbol{\delta}_l. \tag{6}$$

Step 6: Decrement the counter by 1 as $l=l-1$ and repeat from Step 4 to Step 6 while $l\geq 0$.

Step 7: From the original images $I_0(n_1,n_2)$ and $J_0(n_1,n_2)$, extract two image blocks with their centers on $\boldsymbol{p}_0$ and $\boldsymbol{q}_0$, respectively. Estimate the displacement between the two blocks with sub-pixel accuracy using POC-based image matching. Let the estimated displacement vector with sub-pixel accuracy be denoted by $\boldsymbol{\delta}=(\delta_1,\delta_2)$. Update the corresponding point as follows:

$$\boldsymbol{q} = \boldsymbol{q}_0+\boldsymbol{\delta}. \tag{7}$$

The peak value of the POC function is also obtained as a measure of reliability in local block matching. In the proposed FKP recognition algorithm, we employ BLPOC instead of POC to estimate displacement with sub-pixel accuracy [20].

III. FKP Recognition Algorithm

This section presents the conventional FKP recognition algorithms: (A) the FKP recognition algorithm using BLPOC [8] and (B) the FKP recognition algorithm using phase-based correspondence matching [21], and the proposed algorithm.

A. FKP Recognition Algorithm Using BLPOC [8]

This algorithm is based on the global registration of FKP images using BLPOC. The displacement between the two FKP ROI (Region Of Interest) images is estimated using BLPOC and the two images are aligned by the estimated displacement. Then, the common region of the two images is extracted. For example, Fig. 1 (a) and (b) show the registered and input FKP ROI images and Fig. 1 (c) and (d) show their common regions. If the area ratio of the common region to the ROI image is below the threshold, the BLPOC function between the ROI images is calculated. Otherwise, the BLPOC function between the common regions is calculated. Finally, the highest peak value of the BLPOC function is obtained as the matching score between the two images. In this paper, we employ the

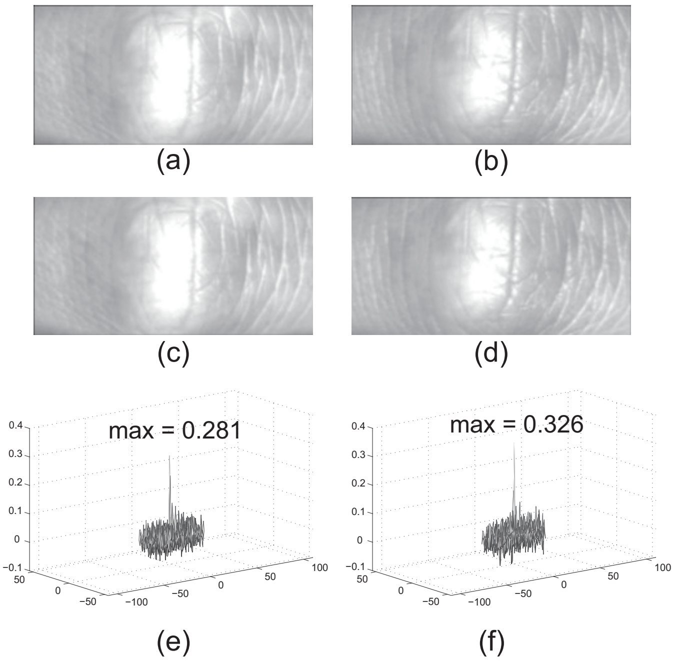

Fig. 1. Example of FKP recognition using BLPOC: (a) input image, (b) registered image, (c) common region of the input image, (d) common region of the registered image, (e) BLPOC function between FKP images (a) and (b) and (f) BLPOC function between common regions (c) and (d).

following parameters: the parameters for the BLPOC function are $K_1/M_1 = 0.25, K_2/M_2 = 0.2$, and the threshold for the area ratio is 0.75. Fig 1 (e) shows the BLPOC function between the FKP ROI images, while Fig. 1 (f) shows the BLPOC function between the common regions. As a result, the use of the BLPOC function between common regions makes it possible to enhance the matching performance compared with the BLPOC function between the original images.

This algorithm considers only the translational displacement between FKP images. So, the recognition performance of this algorithm is significantly dropped for FKP images having nonlinear distortion.

B. FKP Recognition Algorithm Using Phase-Based Correspondence Matching [21]

This algorithm is based on the local registration of FKP images using phase-based correspondence matching and has been successfully applied to palmprint recognition algorithm [21]. The 152 reference points are placed on the registered images and then the corresponding points on the input image are estimated by using the phase-based correspondence matching as shown in Fig. 2 (a) and (b). The BLPOC functions between the reliable corresponding point pairs which similarity is above threshold are calculated, where the threshold is 0.4 in this paper. If the number of the reliable corresponding point pairs is below threshold, we calculate the BLPOC functions for all the corresponding point pairs, where the threshold for the number of reliable corresponding pairs is 133 in this paper. Finally, the matching score is calculated as the highest peak

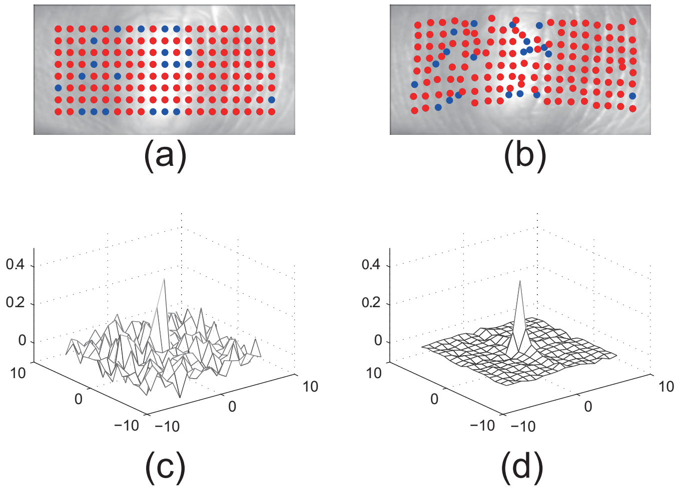

Fig. 2. Example of FKP recognition using phase-based correspondence matching: (a) reference points on the registered image, (b) corresponding points on the input image, where red points indicate that their similarities are above threshold, (c) BLPOC function of a single image block pair and (d) average BLPOC function.

value of the average BLPOC function. To take the average of a set of BLPOC functions, the PNR (Peak-to-Noise Ratio) of the BLPOC function can be improved as shown in Fig. 2(c) and (d). In this paper, the parameters for phase-based image matching are as follows: the number of layer images is 3, the size of local block image is 32×32 pixels, and the parameter of BLPOC function is $K_1/M_1 = K_2/M_2 = 0.5$.

This algorithm can handle the nonlinear distortion of FKP images. However, the phase-based image matching cannot find the accurate corresponding points due to its poor texture on the knuckle region and the large movement of a finger.

C. Proposed FKP Recognition Algorithm

The FKP images have the nonlinear distortion due to the movement of fingers. The proposed algorithm corrects nonlinear distortion of FKP images using the affine transformation and then calculates the matching score.

The 126 reference points are placed on the registered image and the corresponding points on the input image are estimated by using BLPOC-based correspondence matching as shown in Fig. 3 (a) and (b). The parameters of the affine transformation are estimated using the reliable corresponding point pairs. In the case of FKP images, distortion is different between the left and right regions of the knuckle. So, we estimate the parameters of the affine transformation for each region. Fig. 3 (d) and (e) show the distortion corrected images with the affine transformation for left and right regions, respectively. The 18 reference points are placed on the registered image as shown in Fig. 3 (c). The 9 reference points on the left half of the image are for the left region of the FKP image, while the 9 points on the right half of the image are for the right region of the FKP image. The corresponding points on the input image are estimated by using BLPOC-based corresponding matching for left and right regions, respectively. Then, the

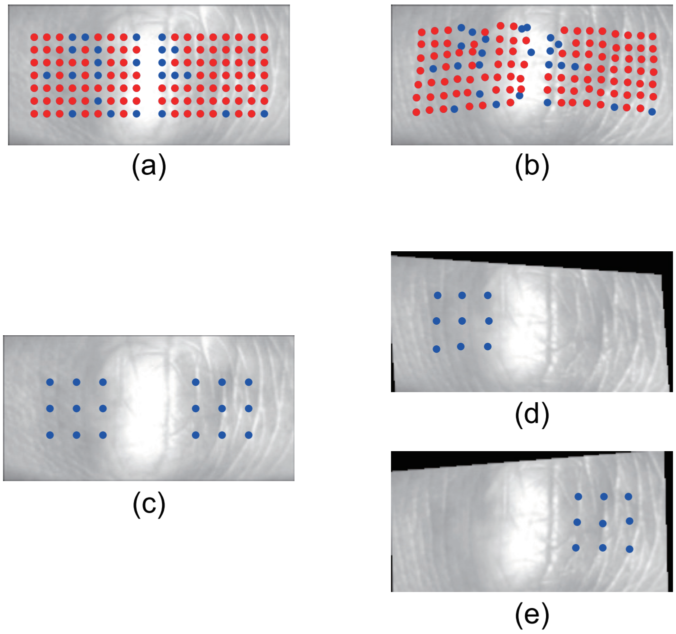

Fig. 3. Example of FKP recognition using the proposed algorithm: (a) reference points on the registered image for distortion correction, (b) corresponding points on input image, where red points indicate that their similarities are above threshold, (c) reference points on the registered image for matching score calculation, (d) left half of the input image after distortion correction and the corresponding points and (e) right half of the registered image after distortion correction and corresponding points.

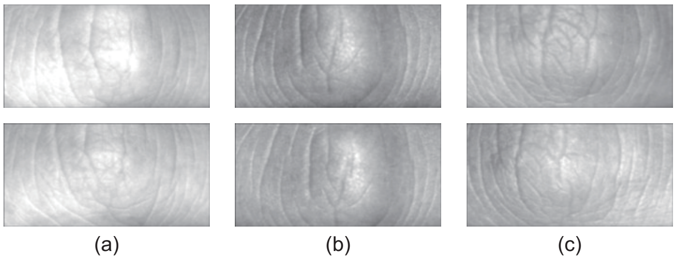

Fig. 4. Examples of FKP ROI images in the PolyU FKP database: palmprint image pairs with different lighting condition (a) and nonlinear distortion (b) and (c).

local block images are extracted according to the position of the corresponding pairs. We calculate the BLPOC function for each local block image pair and take the average of a set of the BLPOC functions. Finally, the matching score between the FKP images is obtained as the highest peak value of the average BLPOC function. In this paper, the parameters for the proposed algorithm are as follows: the number of layers for estimating parameters of the affine transformation and calculating the matching score is 2 and 1, respectively, and the size of local block image is 32×32 pixels, and the parameter of BLPOC function is $K_1/M_1 = K_2/M_2 = 0.5$.

In the proposed algorithm, the structure of fingers is considered to calculate the matching score. It is expected that the proposed algorithm is robust against the nonlinear distortion of FKP images compared with the conventional algorithms.

IV. Experiments and Discussion

This section describes a set of experiments using the PolyU FKP database [15] for evaluating recognition performance of the FKP recognition algorithms described in the above section: (A) the FKP recognition algorithm using BLPOC [8], (B) the FKP recognition algorithm using phase-based correspondence matching [21] and (C) the proposed algorithm.

The PolyU FKP database consists of 7,920 images (384×288 pixels) with 165 subjects and 6 different images for each of the left index finger, the left middle finger, the right index finger and the right middle finger in 2 separate sessions. In the experiment, images in the first session belong to the gallery set, while images in the second session belong to the probe set, where each session consists of 660 (165×4) classes and 3,960 (660×6) images. The size of FKP ROI images is 220×110 pixels. Fig. 4 shows some examples of FKP ROI images in this database. As shown in this figure, FKP images in the database are captured under different lighting condition and have rotation, translation and nonlinear distortion due to movement of a finger.

The performance of the biometrics-based verification system is evaluated by the Receiver Operating Characteristic (ROC) curve, which illustrates the False Rejection Rate (FRR) against the False Acceptance Rate (FAR) at different thresholds on the matching score. We first evaluate the FRR for all the possible combinations of genuine attempts; the number of attempts is 23,760. Next, we evaluate the FAR for all the possible combinations of impostor attempts; the number of attempts is 15,657,840. The performance is also evaluated by the Equal Error Rate (EER), which is defined as the error rate where the FRR and the FAR are equal.

Fig. 5 shows the ROC curves and EERs for each algorithm, and Fig. 6 shows the matching score distributions of genuine and impostor pairs for each algorithm. The EER of the algorithms (B) and (C) is significant low compared with that of the algorithm (A), since the algorithm (A) does not consider the distortion of FKP images. Comparing the algorithm (B) and (C), the matching score distribution of genuine pairs for the algorithm (C) is higher than that for the algorithm (B), and also the matching score distribution of impostor pairs for the algorithm (C) is lower than that for the algorithm (B). This indicates that the algorithm (C) is suitable for recognizing FKP images compared with the algorithm (B), since the algorithm (C) considers both global and local distortion of FKP images to calculate the matching scores between the FKP images.

V. Conclusion

This paper proposed an FKP recognition algorithm using BLPOC-based local block matching. The proposed algorithm can calculate the matching score between FKP images by correcting the global and local distortion of FKP images considering the structure of fingers. The experiments using the PolyU FKP database demonstrate that the proposed algorithm

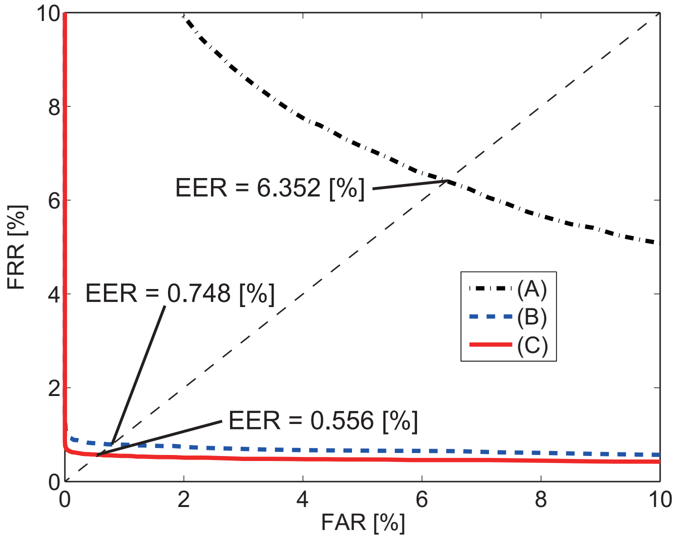

Fig. 5. ROC curves and EERs of the algorithms (A), (B) and (C).

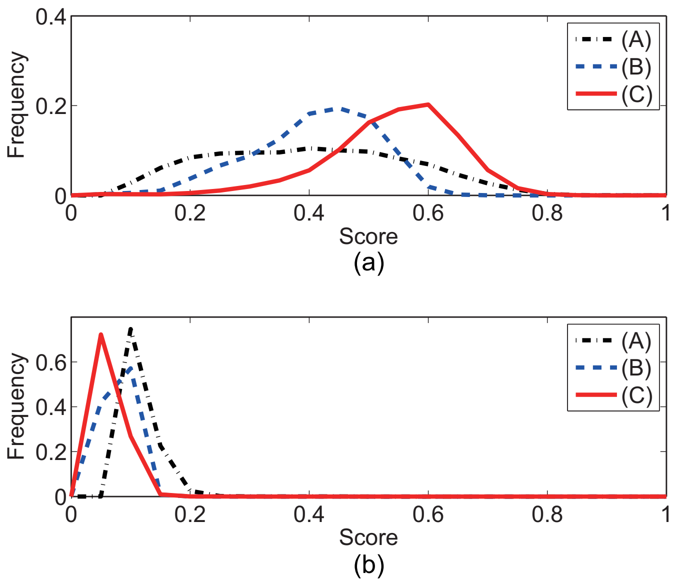

Fig. 6. Matching score distribution for algorithms (A), (B) and (C): (a) distribution of genuine pairs and (b) distribution of impostor pairs.

exhibits higher recognition performance than the conventional algorithms.

References

[1] A.K. Jain, P. Flynn, and A.A. Ross, *Handbook of Biometrics*, Springer, 2008.

[2] D. Maltoni, D. Maio, A. K. Jain, and S. Prabhakar, *Handbook of Fingerprint Recognition*, Springer, 2003.

[3] D. Zhang, *Palmprint Authentication*, Kluwer Academic Publication, 2004.

[4] A. Kong, D. Zhang, and M. Kamel, “A survey of palmprint recognition,” *Pattern Recognition*, vol. 42, no. 7, pp. 1408–1418, 2009.

[5] N. Duta, “A survey of biometric technology based on hand shape,” *Pattern Recognition*, vol. 42, pp. 2797–2806, 2009.

[6] D.L. Woodard and P.J. Flynn, “Finger surface as a biometric identifier,” *Computer Vision and Image Understanding*, vol. 100, pp. 357–384, 2005.

[7] L. Zhang, L. Zhang, and D. Zhang, “Finger-knuckle-print: A new biometric identifier,” *Proc. Int’l Conf. Image Processing*, pp. 1981–1984, 2009.

[8] L. Zhang, L. Zhang, and D. Zhang, “Finger-knuckle-print verification based on band-limited phase-only correlation,” *Lecture Notes in Computer Science*, vol. 5702, pp. 141–148, 2009.

[9] A. Kumar and Y. Zhou, “Human identification using knucklecodes,” *Proc. IEEE Third Int’l Conf. Biometrics: Theory, Applications and Systems*, pp. 1–6, 2009.

[10] L. Zhang, L. Zhang, D. Zhang, and H. Zhu, “Online finger-knuckle-print verification for personal authentication,” *Pattern Recognition*, vol. 43, pp. 2560–2571, 2010.

[11] L. Zhang, L. Zhang, D. Zhang, and H. Zhu, “Ensemble of local and global information for finger-knuckle-print recognition,” *Pattern Recognition*, 2010, (online available).

[12] A. Kumar, D.C.M. Wong, H.C. Shen, and A.K. Jain, “Personal authentication using hand images,” *Pattern Recognition Letters*, vol. 27, pp. 1478–1486, 2006.

[13] G.K.O. Michael, T. Connie, and A.T.B. Jin, “An innovative contactless palm print and knuckle print recognition system,” *Pattern Recognition Letters*, vol. 31, pp. 1708–1719, 2010.

[14] L. Zhu and S. Zhang, “Multimodal biometric identification system based on finger geometry, knuckle print and palm print,” *Pattern Recognition Letters*, vol. 31, pp. 1641–1649, 2010.

[15] PolyU FKP Database, http://www4.comp.polyu.edu.hk/˜biometrics/FKP.htm, ,” .

[16] C. D. Kuglin and D. C. Hines, “The phase correlation image alignment method,” *Proc. Int. Conf. Cybernetics and Society*, pp. 163–165, 1975.

[17] K. Takita, T. Aoki, Y. Sasaki, T. Higuchi, and K. Kobayashi, “High-accuracy subpixel image registration based on phase-only correlation,” *IEICE Trans. Fundamentals*, vol. E86-A, no. 8, pp. 1925–1934, Aug. 2003.

[18] K. Takita, M. A. Muquit, T. Aoki, and T. Higuchi, “A sub-pixel correspondence search technique for computer vision applications,” *IEICE Trans. Fundamentals*, vol. E87-A, no. 8, pp. 1913–1923, Aug. 2004.

[19] K. Ito, H. Nakajima, K. Kobayashi, T. Aoki, and T. Higuchi, “A fingerprint matching algorithm using phase-only correlation,” *IEICE Trans. Fundamentals*, vol. E87-A, no. 3, pp. 682–691, Mar. 2004.

[20] T. Shibahara, T. Aoki, H. Nakajima, and K. Kobayashi, “A high-accuracy stereo correspondence technique using 1d band-limited phase-only correlation,” *IEICE Electronics Express*, vol. 5, no. 4, pp. 125–130, Feb. 2008.

[21] K. Ito, S. Iitsuka, and T. Aoki, “A palmprint recognition algorithm using phase-based correspondence matching,” *Proc. Int’l Conf. Image Processing*, pp. 1977–1980, Nov. 2009.